

Detailed Phase Transition Study at $M_H \leq 70$ GeV in a 3-dimensional $SU(2)$ -Higgs Model

M. Gürtler^{1*}, E.-M. Ilgenfritz², J. Kripfganz³, H. Perlt¹ and A. Schiller¹

¹ *Institut für Theoretische Physik, Universität Leipzig, Germany*

² *Institut für Physik, Humboldt-Universität zu Berlin, Germany*

³ *Institut für Theoretische Physik, Universität Heidelberg, Germany*

We study the electroweak phase transition in an effective 3-dimensional theory for a Higgs mass of about 70 GeV by Monte Carlo simulations. The transition temperature and jumps of order parameters are obtained and extrapolated to the continuum using multi-histogram techniques and finite size analysis.

1. Introduction

One approach to lattice calculations of the electroweak transition is based on an effective 3-dimensional $SU(2)$ -Higgs model. It is attractive phenomenologically because it circumvents the problem of putting chiral fermions on the lattice. Due to dimensional reduction, fermions as well as non-static bosonic modes contribute to the effective action. In contrast to QCD, dimensional reduction should work for the electroweak theory around and above the transition temperature because g^2 is small. For the electroweak phase transition this approach has been pioneered by Farakos et al. (see *e.g.* [2]). In its simplest version the dimensionally reduced effective theory is again an $SU(2)$ -Higgs theory with just one doublet.

2. The lattice model

On the lattice, we study the $SU(2)$ -Higgs system with one complex Higgs doublet of variable modulus. The gauge field is represented by unitary 2×2 link matrices $U_{x,\alpha}$, the Higgs fields are written as $\Phi_x = \rho_x V_x$ ($V_x \in SU(2)$). The lattice action is

$$S = \beta_G \sum_p \left(1 - \frac{1}{2} \text{Tr } U_p\right) - \beta_H \sum_l \frac{1}{2} \text{Tr} (\Phi_x^+ U_{x,\alpha} \Phi_{x+\alpha})$$

$$+ \sum_x (\rho_x^2 + \beta_R (\rho_x^2 - 1)^2) \quad (1)$$

($\rho_x^2 = \frac{1}{2} \text{Tr} (\Phi_x^+ \Phi_x)$, U_p denotes the $SU(2)$ plaquette matrix), with

$$\beta_G = \frac{4}{ag_3^2}, \quad (2)$$

$$\beta_R = \frac{\lambda_3}{g_3^2} \frac{\beta_H^2}{\beta_G} = \frac{1}{8} \left(\frac{M_H^*}{80 \text{ GeV}} \right)^2 \frac{\beta_H^2}{\beta_G}, \quad (3)$$

$$\beta_H = \frac{2(1 - 2\beta_R)}{6 + a^2 m_3^2} \quad (4)$$

(a is the lattice spacing). The lattice model defined by (1) is numerically studied at given couplings β_G, β_H and λ_3/g_3^2 .

In the search for the phase transition, bulk variables like

$$\rho^2 = \frac{1}{L_x L_y L_z} \sum_x \rho_x^2, \quad (5)$$

$$E_{link} = \frac{1}{3L_x L_y L_z} \sum_{x,\alpha} \frac{1}{2} \text{Tr} (\Phi_x^+ U_{x,\alpha} \Phi_{x+\alpha}) \quad (6)$$

are used.

The update is a combination of $3d$ and $4d$ Gaussian heat bath for the gauge and Higgs fields, respectively, and Higgs reflections. Most of the Monte Carlo data have been obtained on QUADRICS parallel computers.

*Contribution presented by M. Gürtler

3. Phase separation, equal weight and mixed phase configurations

As usual, the search for the phase transition point requires extensive application of the multi-histogram technique [3,4].

We have studied the phase transition driven by m_3 . Then the lattice Higgs self-coupling β_R varies with β_H (see (2)). Therefore, the reweighting uses not only E_{link} , but ρ^2 and ρ^4 at the same time.

We have determined the finite volume pseudo-critical $\beta_{Hc}(L)$ by the minima of the Binder cumulants and the maxima of the susceptibilities

$$B_{\rho^2}(L, \beta_H) = 1 - \frac{\langle (\rho^2)^4 \rangle}{3\langle (\rho^2)^2 \rangle^2}, \quad (7)$$

$$C_{\rho^2}(L, \beta_H) = \langle (\rho^2)^2 \rangle - \langle \rho^2 \rangle^2 \quad (8)$$

(in the same way for other observables) as well as using the equal weight method.

The application of the equal weight criterion requires a procedure to separate the (measured or reweighted) histogram into contributions attributed to the pure phases. In addition, there are inhomogeneous (mixed) configurations contributing to the histogram. Our main assumption is that the pure phases can be described by Gaussian distributions for any volume averaged quantity. The normalised histogram has been represented as a weighted sum of three histograms

$$p(\rho^2, \beta_H) = w_b p_b(\rho^2, \beta_H) + w_s p_s(\rho^2, \beta_H) + w_{mix} p_{mix}(\rho^2, \beta_H) \quad (9)$$

with $w_b + w_s + w_{mix} = 1$. $w_{b,s}$ denotes the weight of the broken/symmetric phase, w_{mix} that of the mixed state.

The positions, widths and weights of the pure phase histograms at a given β_H have been obtained by fitting the outer flanks of the two-peak histogram to Gaussian shape. This fixes the weight w_{mix} and the ρ^2 distribution to be attributed to configurations with domains of both phases in equilibrium. The pseudo-critical β_{Hc} is found according to the requirement $w_b = w_s$.

Another kind of phase separation was used to estimate the jump of the plaquette and correlation lengths of "pure" phases at the critical point.

The aim is to remove successful tunneling escapes and unsuccessful tunneling attempts towards the "wrong" phase from what should then be considered as the Monte Carlo trajectory restricted to the "right" phase.

The procedure rescans the records of ρ^2 which has a well separated two-peak signal for all considered volumes. Referring to this variable a lower cut for the upper (broken) phase and an upper cut for the lower (symmetric) phase can be chosen. The cuts are determined in such a way that the remaining histograms (for the "pure" phases) are almost symmetric around their maxima. If the Monte Carlo history of ρ^2 enters the range of a certain phase and stays there for a number of iterations (larger than the autocorrelation time *without* tunneling but smaller than that *with* tunneling), the sequence of configurations is considered to belong to that phase until the trajectory leaves it.

4. Phase Transition Localisation

To demonstrate the two-peak structure we show in Fig. 1 the measured histogram of ρ^2 on lattices 48^3 and 64^3 , all at $\beta_G = 12$, for β_H values nearest to the respective pseudo-critical $\beta_{Hc}(L)$. The positions of the maxima change already only slightly with the volume.

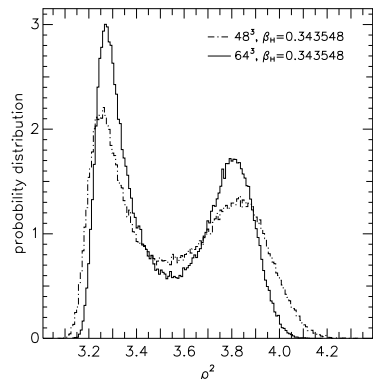


Figure 1. Measured histograms of ρ^2 for $\beta_G = 12$

In Fig. 2 results of the multi-histogram interpolation of our data for $\beta_G = 12$ for the Binder cumulant of E_{link} are presented. Finiteness and shrinking of the Binder cumulant with increasing volume present evidence for the first order nature

of the transition at Higgs mass $M_H^* = 70$ GeV.

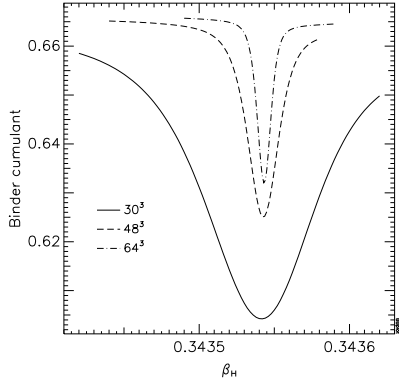


Figure 2. Binder cumulant for E_{link} , $\beta_G = 12$

An equal-weight histogram ($\beta_{Hc}(L) = 0.3435441$) for a lattice size 64^3 is presented in Fig. 3 together with the Gaussians describing the pure phases. The distribution attributed to mixed configurations with domains of both phases in equilibrium is well identified between the two peaks.

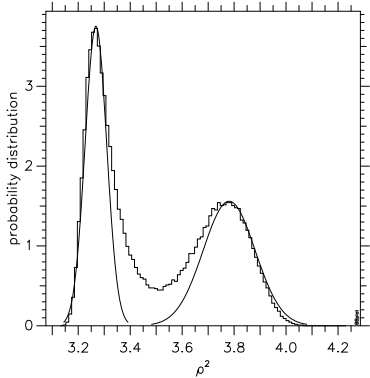


Figure 3. Equal weight histogram

The various pseudo-critical $\beta_{Hc}(L)$ values for the different methods applied to E_{link} and ρ^2 are collected in Fig. 4, plotted versus $1/L^3$ for $\beta_G = 12$. Corresponding to each method, a $1/L^3$ fit has been used to yield a respective β_{Hc}^∞ . The extrapolations nicely coincide as expected.

In Table 1 the extrapolations for each method are collected together with the average β_{Hc}^∞ for $\beta_G = 12$ and 16. The result is translated into a physical temperature and an "exact" Higgs mass M_H using the correspondence to quantities in the

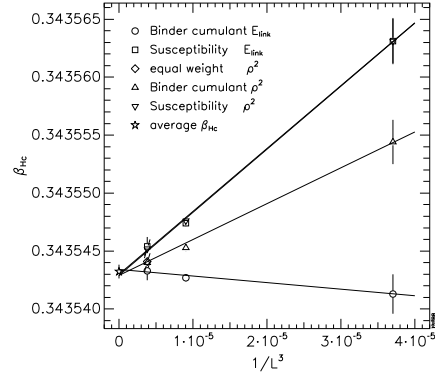


Figure 4. Infinite volume extrapolation of $\beta_{Hc}(\beta_G = 12)$

4-dimensional theory in 1-loop accuracy (no μ_4 -dependence, see [2]).

These numbers are given for the case of the $SU(2)$ -Higgs theory without and with fermions (*i.e.* including the top quark with a mass of 175 GeV). Comparing the temperatures, there seems to be not much space left for $O(a)$ corrections. The "exact" Higgs mass is practically the same.

$\beta_G = 12$	B	C	$w_b = w_s$
E_{link}	0.3435434	0.3435430	
ρ^2	0.3435429	0.3435429	0.3435441
β_{Hc}	0.3435433(6)		
	no fermions	$m_t=175\text{GeV}$	
T_c/GeV	150.94(1)	107.05(1)	
M_H/GeV	64.77	69.42	

$\beta_G = 16$	B	C
E_{link}	0.3407950	0.3407937
ρ^2	0.3407943	0.3407939
β_{Hc}	0.3407942(6)	
	no fermions	$m_t=175\text{GeV}$
T_c/GeV	151.27(1)	107.17(1)
M_H/GeV	64.77	69.46

Table 1. Infinite volume limit for β_{Hc} at $M_H^* = 70$ GeV

For comparison, at the smaller coupling ($M_H^* = 35$ GeV) the transition temperature (without top) is $T_c = 76.2(1)$ GeV with the Higgs mass $M_H = 29.5$ GeV. This has been obtained for gauge couplings in the range from $\beta_G = 12$ to 20 on lattices of size 40^3 and 20^3 [5].

5. Condensate discontinuities

The jumps in $\langle\rho^2\rangle$ and $\langle\rho^4\rangle$ are connected to the renormalization group invariant discontinuities of the quadratic and quartic Higgs condensates. The two-state signal for $\langle\rho^2\rangle$ and $\langle\rho^4\rangle$ is still clearly visible for all lattice sizes considered at the higher Higgs mass of $M_H^* = 70$ GeV, where the transition turns out much weaker than at $M_H^* = 35$ GeV.

Corresponding to the different criteria applied for the definition of the pseudo-critical $\beta_{Hc}(L)$ we obtain histograms of the various operators just at the respective pseudo-criticality. A collection of discontinuities of $\langle\rho^2\rangle$ for various finite lattices (read off from the maxima of the corresponding histograms) is shown in Fig. 5. As in the analy-

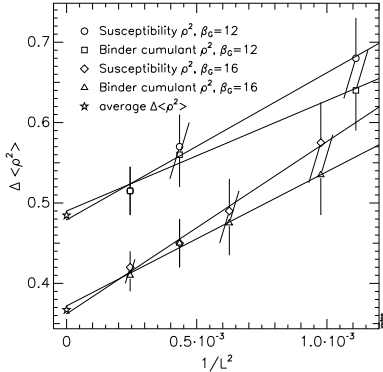


Figure 5. Infinite volume extrapolation of $\Delta\langle\rho^2\rangle$ and $\Delta\langle\rho^4\rangle$

sis of Ref. [6] we found that the size dependence of the jumps for all available lattice sizes is best described by a $1/L^2$ fit. The extrapolation to infinite volume is given in Table 2 in lattice units.

	B_{ρ^2}	C_{ρ^2}	average
$\beta_G = 12$	0.490(9)	0.479(8)	0.485(6)
$\beta_G = 16$	0.372(8)	0.362(7)	0.367(5)
	B_{ρ^4}	C_{ρ^4}	average
$\beta_G = 12$	4.86(9)	4.81(8)	4.84(6)
$\beta_G = 16$	3.62(8)	3.51(7)	3.56(5)

Table 2. Infinite volume limit for $\Delta\langle\rho^2\rangle$ (upper) and $\Delta\langle\rho^4\rangle$ (lower part), $M_H^* = 70$ GeV

Additionally, the expectation value of the average plaquette $\langle P \rangle$ shows a discontinuity as well. This jump is numerically a tiny effect at the larger

Higgs mass. Nevertheless, we are able to estimate it using the phase separation technique discussed earlier.

In Table 3 the jump $\Delta\langle P \rangle$ is reported for β_H values nearest to the critical ones at $M_H^* = 70$ and 35 GeV at lattice sizes 64^3 and 40^3 , respectively.

		$\Delta\langle P \rangle$
$M_H^* = 70$ GeV	$\beta_G = 12$	0.00037
	$\beta_G = 16$	0.00015
$M_H^* = 35$ GeV	$\beta_G = 12$	0.00370

Table 3. Estimated plaquette jump $\Delta\langle P \rangle$

The relation of the measured quantities to continuum physics as well as further consequences are discussed in the related contribution of A. Schiller [7].

6. Summary

We have studied the electroweak phase transition for Higgs masses up to 70 GeV. Its first order nature has been demonstrated. The critical parameters were determined using the multi-histogram technique in conjunction with the equal weight and other more standard criteria giving consistent results. The jumps in several quantities are reported and extrapolated to the continuum.

REFERENCES

1. M. Gürtler, E.-M. Ilgenfritz, J. Kripfganz, H. Perlt and A. Schiller, UL-NTZ 23/96(hep-lat/960542); hep-lat/9512022
2. K. Kajantie, M. Laine, K. Rummukainen and M. Shaposhnikov, Nucl. Phys. **B458** (1996) 90
3. A.M. Ferrenberg and R.H. Swendsen, Phys. Rev. Lett. **61** (1988) 2635; **63** (1989) 1195
4. B. Bunk, E.-M. Ilgenfritz, J. Kripfganz and A. Schiller, Phys. Lett. **B284** (1992) 371; Nucl. Phys. **B403** (1993) 453
5. E.-M. Ilgenfritz, J. Kripfganz, H. Perlt and A. Schiller, Phys. Lett. **B356** (1995) 561
6. K. Kajantie, M. Laine, K. Rummukainen and M. Shaposhnikov, Nucl. Phys. **B466** (1996) 96
7. M. Gürtler, E.-M. Ilgenfritz, J. Kripfganz, H. Perlt and A. Schiller, contribution to LAT-TICE 96